

Decomposing and Executing Serverless Applications as Resource Graphs

Zhiyuan Guo Zachary Blanco Mohammad Shahrade* Zerui Wei
 Bili Dong Jinmou Li Ishaan Pota[§] Harry Xu[§] Yiying Zhang
UC San Diego **University of British Columbia* *§UC Los Angeles*

Abstract

Today’s serverless computing has several key limitations including per-function resource limits, fixed CPU-to-memory ratio, and constant resource allocation throughout a function execution and across different invocations of it. The root cause of these limitations is the “function-centric” model: a function is a fixed-size box that is allocated, executed, and terminated as an inseparable unit. This unit is pre-defined by the cloud provider and cannot properly capture user needs.

We propose a “resource-centric” model for serverless computing that captures fine-grained resource needs throughout an application’s execution using components of distinct resource type, amount, and time span. We build a new resource-based serverless execution platform that executes components in a disaggregated, on-demand, and auto-scaled manner. Our results show that ReSC solves various resource-related issues of today’s serverless computing, while retaining or even improving its performance.

1 Introduction

Serverless computing, commonly offered in the form of Function-as-a-Service (FaaS), is a type of cloud service that allows users to deploy and execute their applications without managing servers. Serverless computing has gained significant popularity in recent years because of its benefits to cloud users: minimal IT burdens and paying only when their applications run.

Despite many benefits, today’s FaaS-based serverless computing still has several key limitations. First, function CPU-to-memory ratios are fixed by providers. Because workloads can have arbitrary CPU-to-memory ratios, fixed ratios result in either CPU/memory wastage (when provisioning for peaks) or performance degradation (when under-provisioned) [17]. Second, a function’s resource reservation is fixed across invocations, but different inputs to the same function could result in different resource requirements [17, 38]. This lack of elasticity would result in resource waste or in the worst case, function failure, if an invocation exceeds the resource reservation. Third, all resources are allocated from the provider at the beginning of a function and kept as long as the function lives. Thus, users have to provision functions for peak usages but

end up not using the peak resources all the time. Meanwhile, data generated during function execution cannot live after execution ends, which makes sharing such data across functions difficult and slow [33, 51]. Finally, the maximum amount of resources a function can use is limited, which can force users to rewrite their large-scale applications like machine-learning inference [11] as smaller pieces that can fit in functions.

Our observation is that the root cause of these limitations is today’s *function-centric* serverless model. A function is a rigid, fixed-size box that couples computing resources as an inseparable unit throughout a function’s execution and across the function’s invocations. If there is any mismatch between an application’s resource need and a cloud provider’s pre-defined function sizes, users will suffer from resource wastage, performance penalty, and/or program rewriting burden.

We argue that we should forgo the function-based execution model and decouple different resource *types* (e.g., CPU vs. memory), different resource *amounts* (e.g., a memory object of 100 MB vs. one of 1 GB), and different *time spans* of resource (e.g., a 1 GB-object that exists in the beginning of a program execution vs. a 1 GB-object at the end) in each invocation of an application. Moreover, these decoupled resource features should follow user applications’ intrinsic needs instead of being pre-defined or limited by cloud providers.

As such, we propose to center serverless computing around the *resource features* of applications, which we call **resource-centric serverless computing**. To concretely demonstrate the feasibility and benefits of resource-centric serverless computing, we build **ReSC**, a serverless computing platform that models and executes applications in a resource-decoupled way. ReSC models an application as a *resource graph*. Nodes in a resource graph represent either a piece of application code (what we call a *compute component*) or one or more data objects (what we call a *memory component*). Each component is associated with three resource features: *resource type*, *resource amount*, and *span*. We set no limit to the amount or time span of a component (within a total user budget cap), and these values can vary across invocations or even within an invocation (e.g., when ReSC auto-scales up a memory component). One component can trigger other components, run in parallel with other ones, or communicate with other

ones (e.g., a compute component access data in a memory component). Users port their applications to ReSC by lightly annotating the original programs or by using libraries that ReSC provides. A ReSC compiler generates a resource graph and components in it from annotated user programs or ReSC library calls; our run-time system dynamically determines the amount and span of a component based on its actual run-time resource needs.

The resource-based serverless model allows great flexibility for capturing user applications’ fine-grained resource needs. However, it introduces a major technical challenge to cloud providers: *allowing arbitrary resource features (type, amount, span) of components could lead to inefficient resource usage* where available resources are “stranded”. Resource stranding happens when a server has some free resource (e.g., 256 MB of memory), but it cannot be used by any workloads because all workloads need more than the free amount (e.g., if the smallest component to be scheduled is 512 MB) or because another type of resource is not free (e.g., no free CPU cycles). Stranded resources can amount to 25% when the load is high in today’s cloud VM instances [35]. Arbitrary resource type, amount, and span could lead to even more resources being stranded. If every allocation unit is the same or is one of a small number of sizes and lasts for a fairly short time period, then resource stranding can be largely avoided. This is the approach taken by today’s FaaS. Unfortunately, such resource limits are the exact cause of FaaS’ problems.

We solve the resource-stranding problem with two system-level ideas, while allowing components in a resource graph to have arbitrary resource features. Our first idea is to *disaggregate* resource types by allocating CPU-type components in a CPU-centric server pool and memory-type components in a memory-centric server pool. By allocating only one type at a time in that type’s pool, we can avoid the need to find a server that has available free amount of every resource type [16, 28], while not imposing any ratio on CPU and memory.

The above disaggregation approach solves the resource type problem, but resource stranding can still happen within a single pool since a component can still have arbitrary amount and span and we allow a component to grow in size. To address this problem, we introduce our second idea: “*materializing*” an arbitrary sized (virtual) component of a type with multiple *fixed-size physical components* of that type. Virtual components capture arbitrary resource needs of an application, while physical components are the actual execution units that have only a few fixed sizes, similar to how memory pages help avoid external fragmentation for arbitrarily-sized virtual memory areas. To further provide tight resource utilization, we dynamically create and terminate physical components in an *on-demand, auto-scaled* manner for each invocation.

Our resource disaggregation and physical component materialization ideas solve the resource stranding problem, but they bring a challenge: performance overhead caused by network delays between physical components. When optimizing

for low cost, our goal is to retain the performance of today’s serverless computing. We solve the performance problem from several perspectives. First, we perform locality-aware scheduling to place frequently communicating components close to each other. Second, we cache/buffer read/write data in a small local cache, and we batch network accesses. Third, we separate control-path operations like network connection establishment from performance critical paths. Fourth, we use a memory-like internal interface to directly access memory components and avoid serialization/de-serialization.

In the worst case where performance overhead is still high after the above optimizations, we propose to merge, or *aggregate*, components that have high communication overhead and run them together in one execution environment in a *balanced pool*, where each server is equipped with similar amounts of CPU and memory resources. We dynamically aggregate and disaggregate components to tune the tradeoff between performance and efficient resource utilization.

We implemented ReSC on top of OpenWhisk [4] and evaluated it with a set of microbenchmarks and two real-world applications: machine-learning model training and data analytics with a TPC-DS benchmark. We compared ReSC to OpenWhisk, AWS Lambda, AWS Step Functions [5], Orion [36], and PyWren [32]. Our machine-learning results show that ReSC reduces resource consumption by 40% to 84% compared to OpenWhisk while only adding 1.3% performance overhead. Our TPC-DS results show that ReSC reduces resource consumption by 16% to 31% and counter-intuitively, improves performance by 15% to 28% compared to PyWren, thanks to our more efficient remote-data accessing mechanism and our better scaling of compute resources.

2 Motivation and Related Work

We now discuss problems of today’s serverless computing resulting from FaaS’ coupled resource type, coupled resource amount, and coupled resource time span.

Coupled resource types and rigid configurations. Today’s serverless offerings deliver functions with rigid CPU and memory configurations. Google Cloud Functions offers only nine CPU-memory configurations [12]. Others offer more configurations, but under fixed compute-to-memory ratios (1 vCPUs to 1,769 MB memory ratio for all AWS Lambda sizes [34]). To choose a good function size, cloud users often times go for lowest dollar cost (correspondingly, the lowest resource consumption). To reduce manual effort, several tools exist to achieve this goal automatically [10, 14, 26, 39]. Although these tools can often find the best cost among provider-offered function sizes, for many applications, none of the provider sizes is the optimal.

To demonstrate this problem, we study two applications in the SeBS benchmark suite [21]: a HTML workload (dynamic-html) and an image recognition workload (image-recognition). We run each workload on our local server in a Docker container that is set to the size combinations of 10 vCPU counts

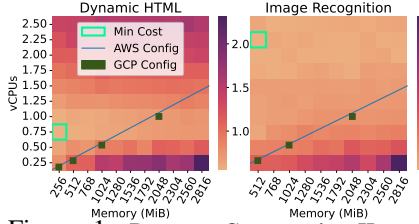


Figure 1: Resource Consumption Heatmap. Each cell runs in a container on a local server with memory and vCPU sizes configured as X and Y axis values. Lighter color is better (smaller cost).

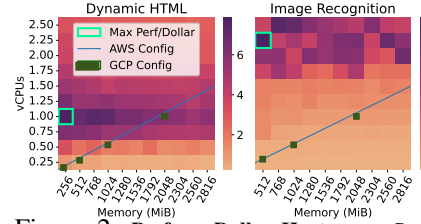


Figure 2: Perf-per-Dollar Heatmap. Performance per dollar calculated using workload execution time and cost as seen in Figure 1. Darker color is better (higher performance per dollar).

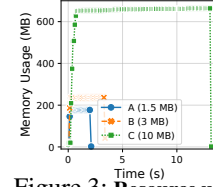


Figure 3: Resource usage with different inputs. Running MP4 add watermark [21].

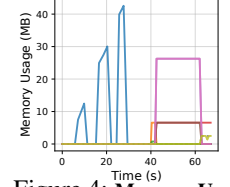


Figure 4: Memory Usage Change over Time. in a Logistic Regression application [19].

and 10 or 11 memory sizes (from the minimal to run the workload to a value that further increasing does not yield benefits). For each configuration, we perform 100 tests and measure the workload’s average execution time. We then calculate the $\text{GB} \times \text{sec}$ and $\text{GHz} \times \text{sec}$ and use Google Cloud (GCP) cost units to get a weighted sum. We plot the resulting value in Figure 1 as heatmaps. We also plot the function configurations AWS and GCP offer. As seen, the minimal-cost sizes do not fall on AWS or GCP’s configurations for either workload. We also plot heatmaps showing perf-per-dollar for the two workloads in Figure 2, as it can be the optimization target for some cloud users. The optimal perf-per-dollar configurations do not fall on AWS or GCP’s configurations either.

Regardless of the optimization goals, fixed CPU-memory configurations cannot meet the diverse demands of applications. A recent work shows that increasing the CPU-memory combinations to 48 and intelligently choosing from them could reduce costs by up to 50% [17]. However, scheduling more CPU-memory sizes creates a harder multi-dimensional bin-packing problem that could result in inefficient resource utilization, a problem that this work does not address. Moreover, this work requires each function to use a single ratio throughout its entire execution and across invocations, which would result in resource wastage as we show next.

Coupled resource amount (across invocations). Today’s cloud providers let users specify the size of a function and use this size for all its invocations. However, an application’s resource demands can vary largely with different inputs [25, 38]. Figure 3 shows the memory usage of a video processing function from [21], which downloads an MP4 video file and adds a watermark to it. We invoke the function with three input videos of 1.5, 3, and 10 megabytes. As shown, for different inputs, the function consumes different amounts of memory. Orion [36] uses execution time distribution history to generate the right size of a function, but this size is set for all invocations of the function.

Coupled resource time span. All resources for a function in today’s serverless platforms have the same time span, as they are allocated in the beginning and released at the end of a function’s execution (or beyond a function’s execution to keep it alive for faster future invocation). This results in resource waste for providers and/or extra costs for users, since a function can often have different phases of resource usages

during execution. For example, Figure 4 shows the memory consumption of several large data structures in a logistic regression program [19] over time. Clearly, this application has different phases of memory consumption.

It is possible to change the billing model to charge for only what is used. For instance, Azure Functions charges based on dynamic memory usage by rounding up to the nearest 128 MB [6]. However, the cloud provider is still left with the incurred cost for the unused resources since all resources are still allocated for the whole function duration [47].

Per-function resource limits. All serverless providers set a limit for the maximum resource consumption of a function. For example, Azure Functions’ Consumption Plan limits application memory to 1.5 GB [6]. Resource limits significantly complicate deploying medium- to large-scale applications such as data analytics [32] and DNN training [59]. The current workaround for hard resource limits is to rewrite user applications by splitting them into smaller pieces each of which fits in a function’s quota [32, 42, 61]. However, with the slow function-to-function communication in today’s serverless platforms, this approach could lead to huge performance overhead. Function resource limits are artificial and have been lifted over time. For instance, AWS Lambda increased the function memory limit from 3,008 MB to 10,240 MB in December 2020, which enabled new applications [1, 2]. However, higher limits could result in more resource wastage because the entire execution might not use the allocated resources. Larger functions also prevents providers from utilizing small free spaces.

Summary. ReSC addresses the limitations stemming from resource coupling and resource caps by decoupling resource type, amount, and time span with no limit to any of them. ReSC dynamically follows an application’s execution needs to allocate the right amount to achieve both low cost and high performance. Meanwhile, ReSC avoids resource stranding with our underlying system that disaggregates resource pools and materializes arbitrary size of application resource needs with fixed-size execution units.

The high-level idea of disaggregating data from compute has been taken by many systems [30, 40, 46, 48, 53]. In fact, serverless functions like Lambda and storage layers like S3 and in-memory storage are a form of disaggregation. Research works on stateful serverless computing like Cloudburst [51],

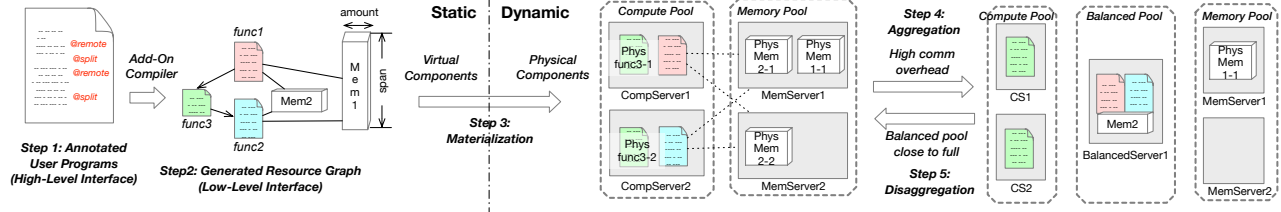


Figure 5: **ReSC Workflow.** This example demonstrates the workflow of ReSC. The user annotates her program with two remote and two split annotations. The ReSC compiler then generates a graph of virtual components. At the run time, ReSC materializes Mem1 as one physical memory component, Mem2 as two physical memory components on two memory servers, two instances of func3 and single instances of func1 and func2 on two compute servers. At a later time, ReSC could decide to aggregate func1, func2, and Mem2 and run them on a balanced server. At yet another time, ReSC could decide to re-disaggregate the components.

Pocket [33], and many more [38, 42, 44, 54] improve the performance and scalability of the disaggregated data layer. However, these systems’ goals are performance, not resource savings. They cannot execute resource graphs as resource-efficiently as ReSC. Beyond our contributions in resource graphs and tools for generating it, the entire ReSC run-time system is designed to execute resource graphs in a more resource-efficient, performant, and flexible way (§5).

3 Resource-Based View of Applications

Different from FaaS-based serverless, ReSC’s view of a serverless application is based on its resource features.

Resource graph. As explained in §1, ReSC models an application as a *resource graph* that contains compute components (code pieces) and memory components (memory objects), with each component having a distinct triad $\langle \text{resource type, resource amount, span} \rangle$. To express the interaction between components, we define two relationships. 1) *triggering*: a compute component triggers one or more compute components. 2) *communicating*: a compute component accesses data in memory components or exchanges messages with other compute components. Note that different from compute components that are explicitly triggered, ReSC automatically starts a memory component when a compute component first initiates an access to it. It ends when the last compute component accessing it ends or explicitly releases it.

A resource graph is neither a data-flow nor a task-flow graph. It captures the distinct resource features of an application. As discussed in §4, ReSC users do not need to define resource graphs or be aware of them. ReSC generates them from user programs and uses them for application execution.

Component materialization. The resource graph described above is intended to follow application resource features to minimize resource wastage. As such, a component in a graph can have arbitrary size and duration. If a system directly schedules and executes them, it would be hard to achieve high utilization of server resources. To solve this problem, we propose to instantiate an arbitrary-sized component as several fixed-size internal components. We call this process *materialization*, the former component *virtual*, the latter *physical*.

ReSC materializes virtual components to physical ones at the run time in an on-demand and auto-scaled fashion that is optimized for run-time scheduling and execution. One virtual

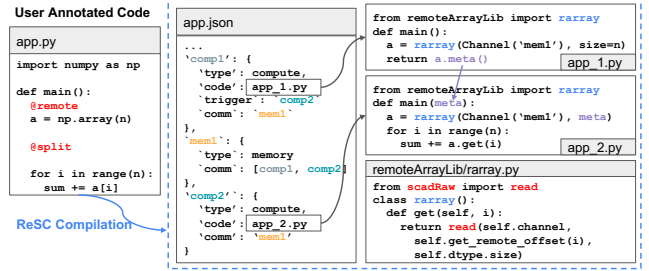


Figure 6: **ReSC Code Example** An annotated user program compiled to the ReSC internal interface. Data structure *a* is placed as a memory object and its lifetime is inferred to span over both compute objects.

component could be materialized as multiple physical components potentially on different servers, and ReSC transparently maps an access of a virtual component to one or more accesses of the corresponding physical component(s). Multiple virtual components could also be materialized as one physical component that runs on one server. ReSC dynamically adds more physical component on demand, e.g., when a virtual memory component’s size grows. It can also create multiple parallel instances of a virtual compute component for better performance. Finally, ReSC dynamically merges (aggregates) virtual components and breaks (disaggregates) merged virtual components based on performance and resource availability.

Decoupling virtual components from physical components allows ReSC’s runtime to 1) avoid resource fragmentation because physical components are all of fixed sizes, 2) transparently and dynamically *scale* a virtual component, 3) have a virtual component’s *size* go beyond what a single machine can hold, and 4) transparently *aggregate* multiple virtual components or *disaggregate* an aggregated component.

4 Porting Applications to ReSC

This section introduces how we port applications to ReSC’s internal resource-graph interface. Our current two approaches serve more as a proof of concept. Future extensions such as profiling-guided resource-graph generation and other compiler optimizations are all possible. Figure 5 illustrates the workflow of ReSC and Figure 6 shows a code example.

User annotation. The first way to use ReSC is by adding simple annotations to original user code: **@split** which indicates a location to separate code into two triggering compute components and **@remote** which indicates a data structure

```

1 # creating a channel
2 chan = Channel('remote-component-name')
3
4 # accessing memory component
5 write(chan, wbuf, addr, size)
6 rbuf = read(chan, addr, size)
7
8 # communication b/w compute component
9 send(chan, wbuf, msg_size)
10 rbuf = recv(chan, msg_size)
11
12 # asynchronous write
13 # other APIs also have an async version
14 id = write_async(chan, wbuf, addr, size)
15 sync(chan, id)
16
17 # management APIs
18 resize(chan, amount) # resizing channel
19 release(chan) # force releasing channel

```

Figure 7: ReSC Low-Level APIs.

that is intended to be placed as a memory component. ReSC compiles user annotated code to an internal representation to be described soon. When compiling, ReSC can identify the relationship between components and the time span (life time) of a component. It also finds the variables that are shared across a `@split` annotation and puts them in a memory component. The compiler then converts the original accesses of these shared variables into ReSC’s internal remote-memory accessing APIs.

ReSC internal interface. The internal interface is fed to ReSC’s execution system. Thus, we design it in such a way to express explicit component graphs and interactions between components. With this internal representation, ReSC’s execution system does not need to directly analyze high-level language or application features. This interface is intended to be used as compiler output or by library and runtime developers. Specifically, the interface is described by a JSON template that specifies virtual compute and memory components and the relationships between them in an application (*i.e.*, one JSON file represents one component graph). Each virtual compute component points to a code piece that is submitted to ReSC together with the JSON file. This interface also includes a set of ReSC low-level APIs as shown in Figure 7 that a compute component code can use to access other memory components or communicate with other compute components.

ReSC libraries. The second way to use ReSC is by replacing existing libraries with ReSC’s corresponding libraries. ReSC libraries implement certain library calls as remote accesses using the internal interface discussed above. As a proof of concept, our current implementation includes two libraries. The *NumPy array* library places a Numpy array annotated with `@remote` as a memory component and implements Numpy array operations to it using ReSC’s internal remote memory accesses. The *DataFrame* library and our compiler convert programs written with pandas [57] to a resource graph. Our compiler generates one memory component per DataFrame and one compute component for each operator such as `map`, `join`, `shuffle`, and `reduce`. The library

implements each DataFrame operator using ReSC’s internal remote-memory accesses. This compiler-library combination demonstrates the possibility of transparently porting programs that are well encapsulated into computation stages.

Application porting. Application developers can leverage their understanding of an application to add annotations or use ReSC libraries. Our simple annotations and proof-of-concept libraries can already support a wide range of programs. New compilers and libraries could be built to support more programs. Application developers can also analyze their applications using profilers like Scalene [8], pprofile [7], or Memray [9] to capture how resource consumption changes and annotate their code accordingly. Future tools and compilers could potentially automate the above steps.

After compiling, users deploy their application to ReSC by submitting the generated JSON file and code pieces. The user also specifies the events which trigger the application. Users can keep adding more or changing existing annotations and library uses to incrementally port their applications to ReSC.

5 ReSC System Design

Figure 8 illustrates the overall architecture of ReSC. A ReSC cluster consists of one or more racks of nodes that belong to one of three *resource pools*: a *compute pool*, a *memory pool*, and a *balanced pool*. While nodes in the compute/memory pool are intended to have more compute/memory than memory/compute resources, nodes in a balanced pool (*e.g.*, Node 2) are similarly equipped with CPU and memory. ReSC places a compute component in the compute pool when its local memory usage is small; when its memory usage grows, ReSC moves it to the balanced pool (§5.3). ReSC places all memory components in the memory pool. ReSC places aggregated components in the balanced pool. ReSC supports different resource disaggregation implementations. For example, resource pools could be physically separated where each node in a pool only serves one resource type. Resource pools can also be virtual, where one node is part of multiple virtual pools (*e.g.*, Node 4).

When a user-specified triggering event happens, our two-level scheduler is invoked with the triggered application’s resource graph. The scheduler decides when and where to execute each physical component. A physical component is then executed in a compute or memory execution environment. Each memory node consists of a *memory controller* that orchestrates the execution of memory components. Similarly, each compute node has a *compute controller* for compute component orchestration. Each controller is responsible for creating, monitoring, and terminating the corresponding components. In addition, each physical server has a *network virtualization component*, which orchestrates component communication. All these three components sit in a user-space *executor* module beneath the actual component execution environments. The executor interacts with the scheduler and other executors. Within the sandbox that hosts a compute

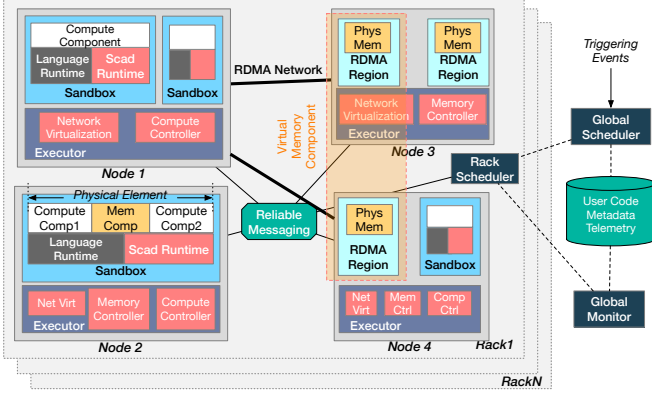


Figure 8: ReSC System Architecture. Node 1 and part of Node 4 belong to the compute pool. Node 3 and part of Node 4 belong to the memory pool. Node 2 is in the balanced pool.

component (Docker container in our implementation), we insert a *ReSC runtime* to handle the ReSC internal APIs for communicating. It also manages a local memory buffer and performs resource and performance monitoring.

The rest of this section presents how ReSC executes resource graphs and decouples resources in a resource-efficient, performant, and flexible way as promised in §2. These include 1) a scheduling system geared towards fast, scalable, and locality-aware allocation of physical components, 2) elastic memory component implementation that minimizes resource stranding, 3) fine-grained, direct remote-memory-access model that fetches data only for the actual accesses and otherwise leaves everything decoupled at memory components, 4) a mechanism to ensure that the compute pool always has minimal and bounded memory use even when a (virtual) compute component grows its memory arbitrarily, 5) a communication mechanism optimized for dynamically added components’ communication, 6) and adaptive ways to adjust resource graph.

5.1 Component Scheduling

We now present ReSC’s scheduler design. Figure 9 plots a startup timeline with three dummy components, with latency of different steps collected when running ReSC.

Two-level scheduler architecture (scalability). Since we materialize a virtual component to potentially multiple physical components, each needing to be scheduled, ReSC needs a scalable scheduler to handle the scheduling load. ReSC adopts a two-level mechanism where a *global scheduler* performs coarse-grained load balancing across racks, and each *rack-level scheduler* performs fine-grained scheduling to map physical components to nodes in the rack. This architecture enables ReSC to handle scheduling requests at a high rate and fits our locality-aware scheduling policy to be discussed soon.

Scheduling policies (performance). Our scheduling policy considers three goals: placing components of a specific type in their corresponding resource pool, placing communicating components close to each other in network distance for better performance, and avoiding cold start as much as possible.

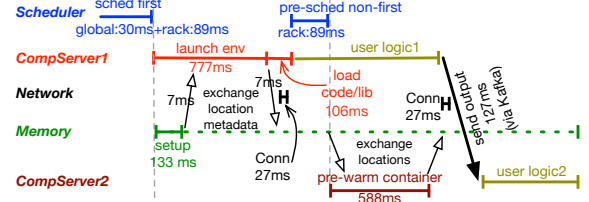


Figure 9: ReSC Startup Flow with Real Results. This example application has two physical compute components accessing one physical memory component; one compute triggers the other compute. Initially, ReSC schedules the first compute and the memory components. They then start their own launch process in parallel. Once the environment is ready, each sends location info to the other; after which RDMA QP (connection) is established. ReSC pre-warms the environment for the second compute component. Dashed green line represents how long the memory component lives.

Thus, our scheduling is *resource-pool aware* and *locality-aware*, in addition to traditional *warm-start awareness*.

Our policy takes the following steps when scheduling a physical component in an application: 1) For the *first* component in a resource graph, we choose a server based on the hash of the application’s and the component’s unique ID to increase the probability of warm start, similar to OpenWhisk (*warm-start aware*); 2) We schedule other *non-first* components in the same rack as previous components that trigger them unless this rack is out of resources, in which case another lightly loaded rack is chosen (*rack-level locality*); 3) If a non-first component has other communicating component(s) that are already running, we schedule it on the same server as one of these other components if the server’s resource permits to exploit *server-level locality* [60]. Otherwise, we fall back to warm-start aware and then to rack-level locality; and 4) For compute components that fail the above steps and for all memory components, we choose a random server that has enough resources in the corresponding resource pool (*resource-pool aware*). As will be seen in §5.2.1, memory components have no application-specific environments and can just be launched on arbitrary servers in the memory pool.

Besides the above policies, we use pre-warming and keep-alive techniques to further avoid cold start of component environments. Specifically, we pre-warm the first component in a resource graph based on historical invocation patterns, similar to previous works [45, 47, 50]. We pre-warm each subsequent component when the previous component is running, similar to Orion [36], as seen in Figure 9.

5.2 Component Execution

Once a component is scheduled, the ReSC execution system is responsible for executing it in an efficient manner and for facilitating its communication with other components. Below, we discuss how Scad executes its memory components and compute components and how it handles component communication and component triggering.

5.2.1 Memory Component Implementation

We now explain how we implement a virtual memory component with dynamically added physical memory components.

Materialization and auto-scaling (cost, no resource limit).

A unique need and challenge in the serverless setting is to quickly react to application resource changes by automatically and transparently adjusting the size of a memory component, while ensuring high resource utilization (*i.e.*, minimal memory stranding). To solve this, our main idea is to materialize each virtual memory component with dynamically added physical components and to use physical memory components as the unit of scheduling and execution environment. Instead of making physical components all of the same size or of arbitrary sizes, we dynamically choose from a small number of configurable sizes for each physical component based on usage patterns (§5.3.1). For example, a 2 GB virtual memory component can be internally represented as two 1 GB physical components or one 1 GB and eight 128 MB ones. This gives ReSC flexibility to balance performance and memory utilization. Currently, 64 MB and 1 GB are the smallest and largest physical memory component sizes in our evaluation, which means ReSC can have at most 1 GB of stranded memory on any server and at most 64 MB for internal fragmentation. These numbers can be configured by system administrators.

To support large, dynamic memory space needs without the upfront commitment of peak memory usage (§2), ReSC automatically scales up a virtual memory component in an on-demand fashion. When starting a virtual memory component, ReSC first allocates and starts a physical memory component with an *initial size*, *e.g.*, 1 GB. As the application allocates more heap memory, ReSC launches more physical components one at a time in an *on-demand* fashion. Each of these physical components is of the same size (what we call *the incremental size*, *e.g.*, 128 MB). ReSC dynamically determines these sizes based on historical memory usage pattern (§5.3.1) and round them up to one of the small number of sizes we support.

Execution environment (performance and safety). Different from traditional serverless functions, memory components only contain data and no computation. Their “execution” just need memory spaces on a server. Thus, we do not use any virtualization environment or containers for them. However, the memory spaces for different memory components should still be properly isolated to prevent one user access other’s data. We rely on either a trusted party (the memory controller or the RDMA hardware) to allocate and manage physical memory component spaces. For example, for RDMA, we assign each physical memory component its own protection domain (PD).

5.2.2 Compute Component Implementation

Two challenges separate ReSC’s compute components from traditional FaaS functions: 1) compute components access data in remote memory and need efficient methods to perform such accesses, 2) we set no limit to how much memory or CPU a compute component can use and thus need mechanisms to auto-scale both memory and CPU of a compute component

to potentially go beyond a single node.

Local memory cache (performance). As many previous memory disaggregation works have shown, a small memory cache at the compute side could largely improve application performance [15, 27, 29, 46, 48]. Similarly, the ReSC runtime transparently maintains a local cache at every compute component. It stores recently read data and buffered writes. The ReSC runtime checks the local cache for remote reads and avoids remote memory accesses if they hit the cache. The runtime buffers asynchronous remote writes (a ReSC internal API) and performs a remote write only when receiving the `sync` command (another ReSC internal API) or when the local cache is full. Currently, ReSC uses a default size of 64MB for the local cache and a cache line size of 4 KB. Future works could improve it with dynamic policies.

Remote-memory access optimization (performance). We optimize remote-memory accesses in our libraries (Numpy and DataFrame), not only for performance but also for reducing memory consumption. Our overall approach is to 1) implement library calls with small working sets, 2) fetch only the working set that will be used right before use and store results back immediately after they are ready, 3) fetch/store data in a batched and asynchronous manner, 4) overlap the data fetching/storing with computation, and 5) avoid serialization/deserialization with direct accesses to remote data structures and zero memory copy. 1) and 2) reduce the local memory usage, while 3), 4), and 5) improve performance. For example, our implementation of the `join` operator fetches a small part of data at a time, by directly reading an offset of a DataFrame from a memory component. When it computes on them, it also initiates the fetching of the next batch of data in the background so that by the time the next batch is about to start the data is already fetched.

Handling local memory pressure (no resource limit).

Physical compute components are intended to use little memory. Thus, we allocate a small and fixed amount (256 MB) for all physical compute components. With this fixed size, there will be no stranding on servers used for the compute pool. However, a virtual compute component can use more memory, as we set no limit to it. To handle this problem, ReSC automatically increases a virtual compute component’s available memory by swapping when the container detects memory pressure. A compute component’s swap space is internally implemented as a set of physical memory components scheduled and executed in the same way as physical memory components for a virtual memory component.

Our remote-memory swapping happens entirely in the user space using Linux `userfaultfd` and is transparent to user applications. Specifically, the ReSC runtime uses a background thread to monitor page faults caused by the user application threads. When a fault happens, if there is not enough swap space, the runtime asks the scheduler to create and launch a new physical memory component. The runtime’s background

thread swaps out pages whenever it detects memory pressure. Since the user-space fault handler cannot access the page table and would not know the page access pattern, we use an NRU (not-recently-used) policy by swapping out a page that has not recently been swapped in.

Scaling compute resources (no resource limit). Apart from scaling up memory resources for a virtual compute component through swapping, ReSC also supports scaling compute resources by triggering multiple parallel instances (*i.e.*, physical compute components) of a virtual compute component. These physical compute components can access (*i.e.*, share) the same set of physical memory components that belong to a virtual memory component. Currently, we do not handle memory consistency and assume that consistency problems either do not happen (*e.g.*, sharded or read-only data) or are handled by user programs. Recent systems like Cloudburst [51] and HydroCache [58] offer casual consistency to serverless functions and can be potentially integrated with ReSC to provide consistency.

5.2.3 Component Communication

Unlike traditional serverless computing, which involves network communication mainly when functions start/terminate, there will be more frequent, intensive communication *during* the execution of disaggregated components in ReSC. In addition, more connection channels need to be established across the finer-grained and dynamically added physical components. Thus, it is crucial to ensure that both the actual communication (data plane) and the connection set up (control plane) are fast.

Control path (performance). When establishing an RDMA connection (*i.e.*, RDMA QP) between two nodes, they need to first exchange a set of metadata describing their own identities. However, two components cannot easily reach each other or establish a connection to perform this initial metadata exchange due to the dynamic and isolated nature of serverless computing. Prior solutions either use a costly overlay network layer (which accounts for nearly 40% of startup time in our experiments or require container runtime changes for performance improvement [52]) or pre-establish all connections [22, 37, 55, 56] (which does not fit our need to dynamically launch memory components). Both approaches try to establish connections via *direct* channels between two nodes.

Our idea is to leverage *non-direct but already established* connections between executors and schedulers to exchange the initial metadata message. Our observation is that a component has always established a connection with its rack-level scheduler by the time when it starts up. Moreover, the scheduler is the one that decides and thus knows the physical locations of the two components that will be communicating. We let the scheduler send one side’s (*e.g.*, *B*’s) physical location (in the form of executor ID) to the other side’s (*e.g.*, *A*’s) *network virtualization module* when initiating the components. Afterwards, *A*’s network virtualization module sets

up and sends the necessary RDMA connection metadata of *A* together with the destination component’s executor ID (*B*) to the scheduler. The scheduler routes the message containing *A*’s metadata to the target executor, which then gets sent to the destination component (*B*) by its network module. After both sides acquire the other’s metadata message, they establish an RDMA QP. The entire QP establishment takes only 34 *ms*.

To further optimize the startup performance, the QP establishment process starts as soon as the execution environment is ready, while user code is loaded in parallel. Doing so hides the QP establishment overhead behind the performance-critical path (Figure 9).

Furthermore, we reuse an RDMA QP when a component tries to establish the communication with a physical memory component located on a server that already has another physical memory component communicating with the component. Since the new and the existing physical memory components are both accessed by the same component, there is no need to isolate them and one QP is enough for both components.

Data path (performance). ReSC’s RDMA communication data path bypasses kernel. When a compute component accesses another component (compiled as an internal communication API), the ReSC runtime looks up which QP it corresponds to. It then issues a one-sided RDMA operation for *read/write* for memory components or a two-sided RDMA operation for *send/recv* for compute components. As one virtual component can be mapped to multiple physical components, if the internal API call touches a memory region that is on two physical memory components, the ReSC runtime dispatches two one-sided RDMA operations to these components and merge the responses. We exploit zero-copy techniques when implementing the data path to improve performance.

5.2.4 Component Triggering and Failure Handling

The communication between triggering components is performed only once — sending the output of a component to its subsequent component as the input. This one-time message is critical for failure handling, as the input can be used for re-execution of a component after its failure. Thus, our goal of triggering component communication is *not performance but reliability*.

To avoid re-executing the entire execution flow after a failure, Scad relies on recording the messages sent between triggering components via a reliable messaging system (*i.e.*, Kafka [31]). When a failure happens at a physical component, we discard the crashed component, all other physical components belonging to the same virtual component, and all this virtual component’s communicating components. We then re-execute from the persistently recorded input messages to these discarded components. This applies to memory components as well. We do not make memory components durable or replicate them, as they only store intermediate state [33]. If a physical memory component crashes, all the compute components that access it and all other physical memory com-

ponents of the same virtual memory component are discarded. If a compute component crashes, the memory components it accesses are all discarded.

Resuming from the reliably recorded messages in the above manner is sufficient to guarantee *at-least-once* semantics, which is the same as today’s serverless systems [20, 49]. If no restarted component modifies external state we can further guarantee *observably exactly-once* semantics. Our failure handling design balances foreground performance and failure recovery performance compared to mechanisms that take more checkpoints [18] or those that restart the entire function chain after a failure [3, 5].

5.3 Component Materialization and Resource Adjust

At any single point, we want to optimize a ReSC cluster to utilize resources available in different pools while improving the overall performance of all executing applications. Meanwhile, for each application, we aim to automatically adjust its resource plan based on historical usage patterns. To achieve these goals, ReSC dynamically sets the default resource plan and “morphs” the resource graph before the invocation of an application.

For each invocation, ReSC collects resource usage for each component and reports it to the global monitor. Instead of using the metrics collected in the current invocation for component adjustment, we incorporate historical resource usages to avoid adjusting components out of one-time input changes.

For component i of the DAG with n_i physical components, the corresponding resource usage vectors of CPU, memory (including remote swap), and network bandwidth are as follows:

$$C_i = [c_1, \dots, c_{n_i}], M_i = [m_1, \dots, m_{n_i}], B_i = [b_1, \dots, b_{n_i}] \quad (1)$$

Storing all resource usage measurements as time series is costly. To keep the metadata overhead low, we only store the exponential moving average (EMA) of measurements. Upon receiving the t^{th} measurements, we update the C vector in the following way (similarly for M and B):

$$C_i^t = \begin{cases} [c_1^t, \dots, c_{n_i}^t], & t = 0 \\ \alpha([c_1^t, \dots, c_{n_i}^t]) + (1 - \alpha)C_i^{(t-1)}, & t > 0 \end{cases} \quad (2)$$

α is a coefficient between 0 and 1 and controls the decay speed of old observations. We use $\alpha = 0.5$ by default.

5.3.1 Per-component Resource Adjustment

As shown later in §6.2.3, it is critical to right-size components to hit a balance between performance and resource efficiency. To do this, ReSC readjusts each component’s resource allocation periodically after K (e.g., 1000) invocations of an application. For a compute component, if the total memory usage (including swap) is below a preset threshold (256MB by default), we leave the component in the compute pool. If the swap frequency of the compute component in the compute

pool is consistently high and total memory footprint exceeds this limit, ReSC moves it to the balanced pool and sets its local memory size to the measured swap space size plus the prior local memory size. For a memory component, the adjustment is its initial and incremental memory allocation sizes (5.2.1). We set these sizes based on historical memory usage patterns.

5.3.2 Component Aggregation

When disaggregated components communicate across the network, aggregating them and running them in a unified environment in the balanced pool eliminates the network communication overhead. Given all sets of communicating components and their network load profile, ReSC needs to pick which sets to aggregate, as the balanced pool has limited space that cannot fit all aggregated components. We frame this problem as a *zero-one* integer linear program (ILP) where each candidate is decided to be aggregated (1) or not (0). Each aggregation candidate is represented by its component-to-component network communication matrix, and its components’ CPU and memory usage vectors. The ILP solver assigns the binary decision variables such that the total network communication overhead is minimized (optimization function), while respecting the available resources in the balanced pool (constraint).

After aggregating two or more components, they become a new physical component that runs in one sandbox and is a single unit that the ReSC scheduler schedules. When merging a compute component with one or more memory components, we allocate one or more ReSC-managed memory spaces inside the merged sandbox. Each such memory space represents an original memory component and is initiated to its estimated size. During execution, ReSC’s runtime handles internal memory access calls from the compute component by memory copying to/from the local memory space. When merging K compute components, the ReSC runtime starts K processes in one sandbox, each running a corresponding code piece. It handles communication API calls by sending/receiving inter-process messages. Giving each merged component its own space allows ReSC runtime to monitor the communication load between the original components, while having merged components run in one sandbox improves performance [24].

5.3.3 Component Disaggregation

When the balanced pool gets overloaded, ReSC needs to disaggregate to free up resources. Determining which disaggregation candidate to choose is also done using a zero-one ILP solver. Here the goal is to incur minimum increase in network communication overhead (optimization function), while respecting the resources available in memory and compute pools (hard constraints) and freeing up a minimum amount of resources from the balanced pool (soft constraint). Note that our aggregation mechanism discussed in §5.3.2 is what enables us to still capture the communication load between components after they are aggregated.

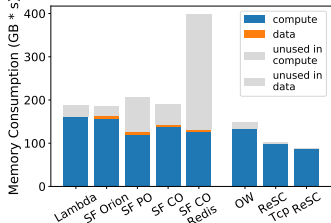


Figure 10: Memory Consumption for LR with largest input dataset.

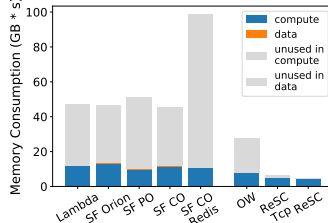


Figure 11: Memory Consumption for LR with midsize input.

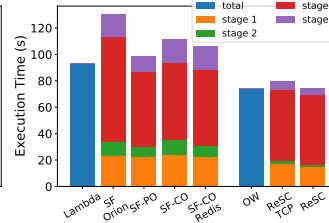


Figure 12: Execution Time Breakdown for LR.

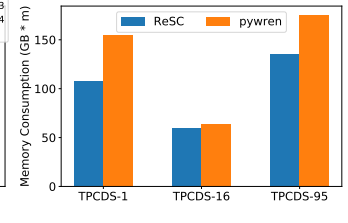


Figure 13: Memory consumption of TPC-DS.

6 Evaluation

We implemented ReSC on top of Apache OpenWhisk [4]. Currently, ReSC supports programs written in Python, the most commonly used programming language in serverless [23]. In total, Scad includes $\sim 15K$ SLOC: 8K lines of Scala to extend Openwhisk’s scheduler and executor, and 4K lines of C together with 1.8K lines of Python for runtime and libraries. We evaluated ReSC on a local cluster of 8 servers, each of which is a Dell PowerEdge R740 equipped with an Intel Xeon Gold 5128 CPU, 64 GB of memory, and a 100 Gbps Mellanox Connect-X5 NIC. All the servers are connected to a 100 Gbps FS N8560-32C 32-port switch. All servers run Ubuntu v20.04 with Linux v5.4.0. We use Docker v20.10.6 for containers.

6.1 Applications

We first present the results of running two applications on ReSC and other systems in comparison.

6.1.1 Logistic Regression (LR) Training

Our first application is a machine learning training task using logistic regression (LR) ported from Cirrus [19]. It first loads the input data set and separates it into a training set and a validation set. Then it performs the regression on the training set. Finally, it validates the trained model with a validation set. We annotate the original code with 3 `@split` annotation points at where tasks change. The compiler generates a graph of four compute components (loading, data-set splitting, training, and validation) and three memory components (training set, validation set, and learned weights).

For this application, we compare ReSC (running RDMA and running TCP) with executing the original program on vanilla OpenWhisk as one function sized to the peak memory size of the program; both systems run on the same local cluster. We also ran a set of configurations on AWS: 1) running the entire program as one Lambda function, 2) running the same four code pieces as ReSC compute components in four Lambdas orchestrated by AWS Step Functions [5] and saving memory components in S3 or in Redis [43] running on an EC2 t3.medium instance. For 2) we use three settings to set function sizes: *SF-PO* (performance optimized): find the optimal performance on Lambda for each function and use the smallest size that can achieve the optimal performance; *SF-CO* (cost optimized): find the Lambda size that results in the lowest cost [10, 14, 26]; *SF-Orion*: using Orion [36] to

generate the size of each function. Although we only compare with AWS, the problems we show prevail in other clouds.

Figures 10 and 11 plot the total memory consumption of these schemes when processing two input dataset sizes, 12 MB and 44 MB. We separate the accounting of consumption at the compute side (Lambda, ReSC compute components) and the memory side (S3, Redis, ReSC memory components). As all schemes use the same number of vCPUs, CPU consumption comparison directly translates to comparing execution time, which we show in Figure 12.

ReSC cost and performance. For the two inputs, ReSC (when running on RDMA) reduces resource consumption by 40% and 84% compared to OpenWhisk while only adding 1.3% performance overhead. Even when running on TCP, ReSC still largely reduces resource consumption with small performance overhead. Moreover, ReSC only has 0.9%-3% unused resources, while OpenWhisk wastes 9%-70%.

Step function cost and performance. When running the same code pieces on Step Functions with four Lambda functions, the total resource consumption only reduces by 2%-5% with SF-CO and by 3%-3.5% with SF-Orion, far from how much ReSC reduces over OpenWhisk. Digging deeper, we found that splitting a program into Lambda functions introduces both performance and resource overhead, as seen in Figure 12. Each function needs extra time to read/write data from S3 and serialize/deserialize the data. Serialization and deserialization also requires extra memory space. Moreover, the communication between Lambda and S3 is slow. However, communication speed to S3 is not the main performance overhead, as can be seen from the only-slightly-better run time when running on Redis, an in-memory key-value store. These results demonstrate that simply splitting a program on today’s serverless platform is not enough for achieving cost and performance goals.

Resource wastage on AWS. Figures 10 and 11 also report allocated but unused resources (*i.e.*, resource wastage). All AWS-based schemes have huge resource wastage, especially with the small input. There are multiple causes of resource wastage on AWS. First, AWS (and all other public clouds) only allows one function size for all invocations. Users must provision for larger invocations and pay for resource wastage during smaller invocations. Second, Lambda wastes resources because its size has to be set to at least the peak memory size, but at non-peak times, resource is wasted. Third, memory is

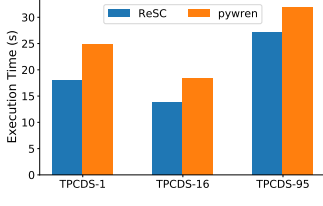


Figure 14: Execution Time of TPC-DS.

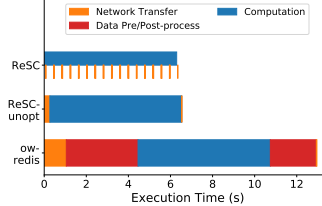


Figure 15: Runtime Breakdown of Reduce-By Op.

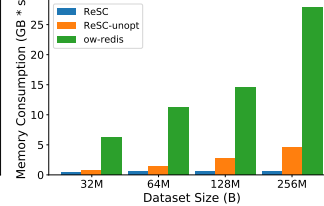


Figure 16: Memory Consumption when Scaling Input Size.

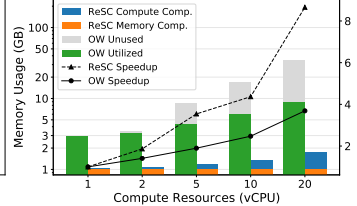


Figure 17: Memory Usage (Log Scale) and Performance Speedup.

wasted when a function reads/writes data from storage and serialize/deserialize them. Fourth, CPU and memory sizes have fixed ratio. When optimizing for performance, the CPU size fits the needs but memory will be over-provisioned, causing more resource wastage in SF-PO. In contrast, when we set the size to be minimal memory, execution time increases significantly (not shown in the figures). Finally, the Redis instance is provisioned for the peak resource usage and wastes huge amounts of resources at non-peak times.

6.1.2 Distributed Queries with TPC-DS

The second application we evaluate is distributed data analytics ported from the PyWren implementation of the TPC-DS benchmark [41]. PyWren splits each TPC-DS query into several stages, each containing some DataFrame operators. For each stage, PyWren generates different amount of workers to perform the computation. Each worker fetches the data to be accessed from an intermediate storage layer (Redis in our evaluation) before the computation starts and stores the data back after the computation finishes.

To port this application, we use the ReSC DataFrame compiler and library (§4) to convert DataFrame operators into compute components and accessed DataFrame objects into memory components. Since with our library, DataFrame operators can directly access remote memory as computation progresses, we remove the explicit data fetching/storing steps in PyWren (except for the first and the last operator which still loads/stores data from Redis hosting the original database).

We use a database size of 100 GB and evaluated three TPC-DS workloads with different performance characteristics and varying resource requirements: queries 1, 16, and 95. They read 2.5 GB, 20 GB, and 19 GB of data respectively and use 6 to 8 compute components and 4 to 6 memory components.

Overall cost and performance. Figure 13 plots the total memory consumption of ReSC and PyWren. For queries 1 and 95, ReSC reduces memory consumption over PyWren for two reasons. First, different operators in a stage need different amounts of memory. With FaaS, PyWren has to provision for the peak memory (2 GB in these cases), while ReSC autoscales the memory component sizes to closely follow the dynamic needs. Second, OpenWhisk pays for $2\times$ memory space when it fetches the entire dataset to the local node and has the same dataset in Redis. ReSC only fetches the data that is needed for a short phase of computation *at the time when it is needed*. We further optimize memory consumption

with our zero memory copy design. For Query 16, ReSC and PyWren consume similar amounts of memory. The majority of this query’s execution time is on its first operator. For the first operator, both ReSC and PyWren fetch the initial data from the Redis database and thus consume similar memory amounts.

Figure 14 plots the total run time of the three queries. ReSC improves performance over PyWren by 15% to 28%, mainly because of ReSC’s avoidance of data serialization and our better speed up when executing parallel compute instances, as explained below.

Closer look at performance. To further understand ReSC’s performance gain, we take a closer look at the 4th stage (Reduce-By-Key) in Query 1 (other queries behave similarly). Figure 15 shows the latency breakdown time line of the execution this stage (excluding container environment startup time). OpenWhisk’s performance is much worse than ReSC mainly because of its data pre- and post-processing, including serialization, data-set partitioning, and de-serialization. In contrast, ReSC internally uses a memory model to directly read/write remote memory into/from local data structures, without the need for any serialization or memory copying. ReSC’s RDMA-based network also contributes to faster network transfer. Finally, ReSC’s library optimization (§5.2.2) further improves the performance over Scad-unopt by reading/writing remote memory in an asynchronous and batched manner, effectively hiding almost all the network communication and setup overhead behind foreground computation.

Independent scaling of compute and memory. To demonstrate ReSC’s ability to independently scale compute and memory resources, we take a closer look at the Reduce-By-Key stage. Figure 16 plots the memory consumption of computational function when we change the input dataset size, while fixing the compute resources to 20 vCPUs. When input data size increases from 64 MB to 1 GB, ReSC’s memory size increases by 1.1 GB, while OpenWhisk’s increases by 3.6 GB. Both systems can use different amounts of memory with the same number of vCPUs (*i.e.*, scaling memory without scaling compute). OpenWhisk’s memory consumption is higher than ReSC because OpenWhisk requires more memory and execution time to load/store data for each function, and the loaded data occupies memory for the entire duration of a function. ReSC directly accesses data in memory nodes at the time when the data is needed.

We then evaluate ReSC’s ability to independently scale

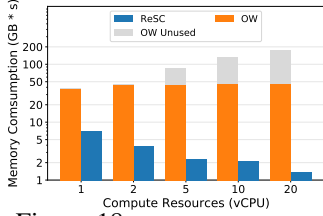


Figure 18: Memory Consumption (log scale) When Scaling Compute Cores.

System Configurations	Time
OpenWhisk	773 ms
OpenWhisk + Overlay	1188 ms
ReSC + Overlay	1002 ms
ReSC no overlay	595 ms
Full ReSC (pre-warm)	284 ms
AWS Lambda	140 ms
AWS Step Functions	215 ms
AWS warm	114 ms
OpenWhisk warm	35 ms
ReSC warm	10 ms

Table 1: Cold and Warm Startup Time.

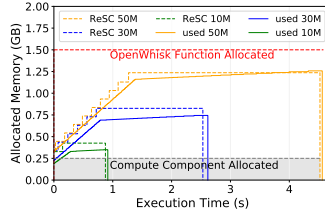


Figure 19: Memory Elasticity. For three different input sizes.

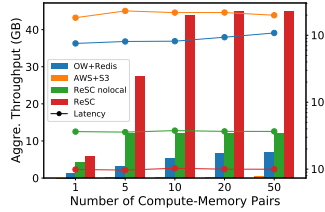


Figure 22: Effect of ReSC Local Scheduling.

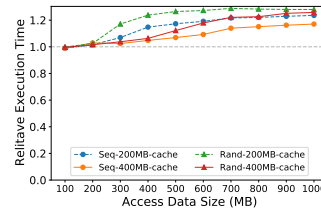


Figure 20: Elastic Compute. With different local memory size.

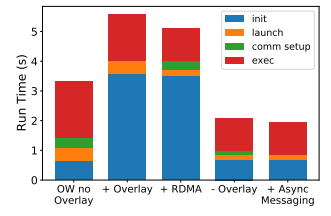


Figure 21: Effect of ReSC's Techniques on Run Time.

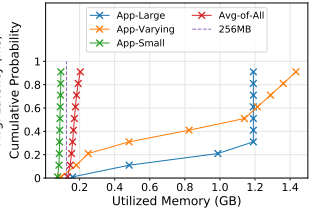


Figure 23: Resource Distribution in Adjustment Experiment.

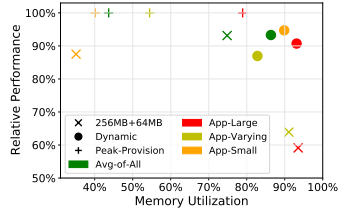


Figure 24: Resource Adjustment. More top-right is better.

compute resources. For this experiment, we use an input data of 1 GB for all the configurations. Figure 17 plots the memory usage and run-time speedup when increasing compute resources (in vCPUs). To model AWS's resource configuration, we set each OpenWhisk function's CPU and memory to have a fixed ratio of 1 vCPU to 1,769 MB memory. OpenWhisk scales out by triggering more parallel instances of a function. Because of the fixed-coupling of CPU and memory, this scaling results in $20\times$ provisioned memory when amount of vCPUs increases by $20\times$. In contrast, ReSC scales only its compute component by invoking 1 to 20 instances of it, while using the same number of memory components. As a result, ReSC's total memory size only increases by 67.4% when its CPU resources increase by $20\times$. For OpenWhisk, in addition to provisioned memory size, we also measure the amount of memory that is used during function execution. Its used memory increases by $2.05\times$, which is much lower than the $20\times$ increase in its provisioned memory. This is because the total amount of processed data is the same when scaling out.

ReSC also achieves a much higher speedup than OpenWhisk when scaling out, because it avoids function performance overheads such as serialization and data partitioning. Because of the high speedup and minimal memory consumption, ReSC's total memory consumption ($\text{GB} \times \text{min}$) decreases by 81% when scaling up, while OpenWhisk's provisioned memory increased by $4.57\times$, and used memory increased by 21.6% as shown in Figure 18.

6.2 Micro-benchmarks

Auto-scaled memory components. To demonstrate how ReSC dynamically scales memory, we build a simple video processing workload that loads a compressed DataFrame dataset, performs random sampling on the dataset, and returns the sampling results. Figure 19 shows the amount of

memory actually used by the workload, memory allocated by ReSC, and memory allocated by OpenWhisk. When calculating ReSC's memory consumption, we also include the local memory used by compute components, which is a fixed but small amount (shown at the bottom of the figure). ReSC closely follows the real memory usage by adding more physical memory components as memory usages increase. In contrast, containers in OpenWhisk (and public clouds like AWS) has one memory size throughout the execution, and the size needs to be provisioned for the peak usage. In this case, the nearest OpenWhisk can provision is 1.5 GB.

Auto-scaled compute components with memory swapping

To measure our swap system performance, we use a simple microbenchmark of sequentially or randomly reading an array of different sizes. Figure 20 plots the total run time of the microbenchmark with increasing array size. We test two local cache sizes: 200 MB and 400 MB, and compare the swap performance against the case where the local memory is larger than the whole array size (*i.e.*, no swapping and the ideal performance but impossible with the compute pool configuration). Overall, swapping only adds 1% to 26% performance overhead. The overhead is higher when the array size is bigger and when the local memory size is smaller.

6.2.1 Component Communication

To understand the impact of ReSC's communication techniques, we run a workload with one compute component accessing one memory component in warm started environments that have not established any connections. Figure 21 demonstrates the effect as we add more techniques to the baseline. The first bar is the baseline OpenWhisk without an overlay network (and thus cannot support dynamic component-to-component communication). The second bar adds the overlay network (so that components can directly communicate with each other); the overlay network increases the initialization

time. The third bar replaces the TCP stack in the second bar with our RDMA stack, which improves the component execution time but also adds a small communication set up time. The fourth bar removes the overlay network and uses our network virtualization module, which reduces the initialization time. The final bar includes our asynchronous messaging optimization and hides the network connection setup time.

6.2.2 Component Launching and Scheduling

Startup time. To measure startup time, we create an application graph with 10 distinct compute components in a chain, each sleeping for 100 *ms*. We launch the application and measure the end-to-end latency across a variety of systems, each with over 20 trials. Table 1 shows the warm and cold startup time. All the rows except for AWS run on our local cluster. Similar to Figure 21, the overlay network adds significant overhead to the cold startup time for both OpenWhisk and ReSC. ReSC’s pre-warming mechanism further reduces the cold start time. AWS in general has better cold start performance than OpenWhisk-based systems including ReSC because of its lightweight virtualization mechanism [13]. OpenWhisk and ReSC use Docker, which is much slower to start up. Optimizing virtualization for serverless computing has been well studied and is out of scope for this paper.

ReSC’s warm startup time improves by more than 90% over AWS and 71% over OpenWhisk, because ReSC moves scheduling operations off the performance critical path.

Locality-aware scheduling. ReSC’s locality-aware scheduling aims to put communicating components as close to each other as possible. Figure 22 demonstrates the effect of our scheduling and puts it in perspective with running OpenWhisk and Redis on our local cluster and running on AWS Lambda with S3. We also evaluate ReSC without using the locality-aware scheduling (ReSC_nolocal). The workload launches 1 to 50 compute-memory-component pairs. Since ReSC always tries to put communicating components on the same server, its aggregated communication throughput is much higher and the average latency is lower than all other schemes. ReSC also scales better than Redis and ReSC_nolocal by utilizing local network bandwidth. As expected, S3’s performance is the worst (almost invisible in the figure).

Scheduler Scalability We evaluate the maximum throughput of ReSC’s rack-level scheduler and find that it can handle around 20K scheduling requests per second. This scheduling rate is similar to OpenWhisk’s scheduler. However, thanks to our locality based design with a scheduler-per-rack, the number of total messages that the system can handle scales linearly with the number of racks. We also find the request rate to the top-level scheduler to be light (around 50K requests per second) and is never the bottleneck in the system.

6.2.3 Component Adjustment

Per-input component adjustment. We evaluate the effect of our dynamic adjustment of the initial and incremental memory

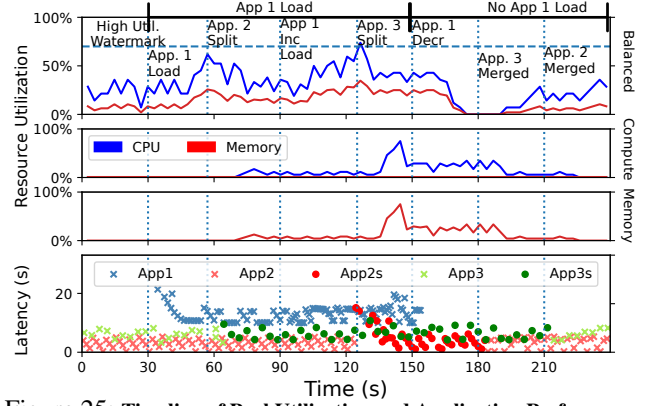


Figure 25: **Timeline of Pool Utilization and Application Performance.** Crosses represent aggregated execution. Dots represent disaggregated execution (App2s and App3s).

component sizes (§5.3.1) using real-world serverless application memory usage profiles from Azure [47]. This dataset contains a set of real-world applications, each being invoked many times with different user inputs. In addition to the average of all the dataset, we choose a few representative applications to highlight. *Small*: most invocations’ memory usages are small, *Large*: most invocations used a lot of memory, and *Varying*: different invocations’ memory usages vary largely. Figure 23 shows the four selected applications’ memory utilization distribution across invocations. For comparison, we also plot a straight line of 256 MB, which is the default initial memory allocation size in ReSC.

Figure 24 plots the performance and memory utilization with three schemes: fixing initial and incremental sizes to 256 MB and 64 MB, provision memory components to the highest usage (peak-provision), and our dynamic adjustment policy. Overall, our dynamic policy achieves high utilization and good performance. Peak provisioning achieves the best performance, since no auto-scaling or swapping is needed, but with low memory utilization. A fixed configuration can lead to both poor resource utilization and poor performance.

Component aggregation and disaggregation. We run three applications concurrently on our cluster configured with a memory pool, a compute pool, and a balanced pool, as shown in Figure 25. App1 is a compute component that cannot be disaggregated. App2 and App3 each has a compute and a memory component that can either be aggregated or disaggregated. Communication between App3’s components is much higher than App2’s. At $t = 0$, App2 and App3 are invoked at steady rate as warmed, aggregated components. As we trigger invocations of App1 from $t = 30$ to $t = 150$, the utilization of the balanced pool reaches the high utilization watermark (70% in this experiment), and ReSC’s disaggregation policy gets triggered at $t = 63$. It decides to disaggregate App2 first since based on history, it has a lower communication load than App3. Doing so is enough to bring the utilization beneath the watermark. As App1’s invocation rate continues to rise, at $t = 117$, the disaggregation policy gets triggered again and ReSC chooses to disaggregate App3. The invocation rate

of App1 decreases from $t = 150$ to $t = 240$, which frees up space in the balanced pool. As a result, our policy decides to aggregate App3 and then App2.

Aggregation improves performance of App2 by 26% and App3 by 5%. Running both applications in an aggregated fashion (§5.3.2) have only less than 2% performance overhead compared to a non-split version of the programs (original programs without any code split). Note that we artificially make App2 to be extremely communication-intensive, which is rare in reality. Aggregating other applications shows an average performance improvement of 14%.

Solver Performance. We implemented the solver using the highly efficient Python Mixed-Integer Linear Program (MIP) package. Finding the optimal solution for 10000 disaggregation candidates each with 32 components takes 10ms-15ms.

7 Conclusion

We present ReSC, a resource-centric serverless computing framework that represents an application as a resource graph and executes the graph in a resource-efficient and performant manner, as shown in our evaluation results. Future works can extend ReSC by adding more features like consistency.

References

- [1] tibanna Documentation. Technical report, Tibanna, April 2021. https://tibanna.readthedocs.io/_/downloads/en/latest/pdf/.
- [2] Using Driverless AI. Technical report, H2O.ai, April 2021. <http://docs.h2o.ai/driverless-ai/latest-stable/docs/userguide/UsingDriverlessAI.pdf>.
- [3] Apache OpenWhisk Composer, Accessed 2022-04-16. <https://github.com/apache/openwhisk-composer>.
- [4] Apache OpenWhisk: Open source serverless cloud platform, Accessed 2022-04-16. <https://openwhisk.apache.org/>.
- [5] AWS Step Functions, Accessed 2022-04-16. <https://aws.amazon.com/step-functions/>.
- [6] Azure Functions Pricing, Accessed 2022-04-16. <https://azure.microsoft.com/en-us/pricing/details/functions/>.
- [7] pprofile: Line-granularity, thread-aware deterministic and statistic pure-python profiler, Accessed 2022-04-16. <https://github.com/vpelletier/pprofile>.
- [8] Scalene: a high-performance CPU, GPU and memory profiler for Python, Accessed 2022-04-16. <https://github.com/plasma-umass/scalene>.
- [9] Memray, Accessed 2022-04-20. <https://github.com/bloomberg/memray>.
- [10] Aws lambda power tuning, Accessed 2022-12-11. <https://github.com/alexcasalboni/aws-lambda-power-tuning>.
- [11] ML inference using Lambda’s 10 GB ephemeral storage, Accessed 2022-12-11. <https://bitesizedserverless.com/bite/ml-inference-in-lambda/>.
- [12] Google Cloud Functions Pricing, Accessed 2022-12-12. <https://cloud.google.com/functions/pricing>.
- [13] Alexandru Agache, Marc Brooker, Alexandra Iordache, Anthony Liguori, Rolf Neugebauer, Phil Piwonka, and Diana-Maria Popa. Firecracker: Lightweight Virtualization for Serverless Applications. In *17th USENIX Symposium on Networked Systems Design and Implementation (NSDI ’20)*, Santa Clara, CA, February 2020.
- [14] Nabeel Akhtar, Ali Raza, Vatche Ishakian, and Ibrahim Matta. COSE: Configuring Serverless Functions using Statistical Learning. In *IEEE INFOCOM 2020 - IEEE Conference on Computer Communications*, 2020.
- [15] Emmanuel Amaro, Christopher Branner-Augmon, Zhihong Luo, Amy Ousterhout, Marcos K. Aguilera, Aurojit Panda, Sylvia Ratnasamy, and Scott Shenker. Can far memory improve job throughput? In *Proceedings of the Fifteenth European Conference on Computer Systems (EuroSys ’20)*, New York, NY, April 2020.
- [16] Yossi Azar, Ilan Reuven Cohen, Seny Kamara, and Bruce Shepherd. Tight Bounds for Online Vector Bin Packing. In *Proceedings of the Forty-Fifth Annual ACM Symposium on Theory of Computing (STOC ’13)*, Palo Alto, California, USA, 2013.
- [17] Muhammad Bilal, Marco Canini, Rodrigo Fonseca, and Rodrigo Rodrigues. With great freedom comes great opportunity: Rethinking resource allocation for serverless functions. *arXiv preprint arXiv:2105.14845*, 2021.
- [18] Sebastian Burckhardt, Chris Gillum, David Justo, Konstantinos Kallas, Connor McMahon, and Christopher S. Meiklejohn. Durable functions: Semantics for stateful serverless. In *Proceedings of the ACM on Programming Languages (OOPSLA ’21)*, New York, NY, October 2021.
- [19] Joao Carreira, Pedro Fonseca, Alexey Tumanov, Andrew Zhang, and Randy Katz. Cirrus: A serverless framework for end-to-end ML workflows. In *Proceedings of the ACM Symposium on Cloud Computing (SoCC ’19)*, November 2019.
- [20] Google Cloud. Cloud Functions execution environment - execution guarantees, Accessed 2022-04-16. <https://cloud.google.com/functions/docs/concepts/exec>.

- [21] Marcin Copik, Grzegorz Kwasniewski, Maciej Besta, Michal Podstawski, and Torsten Hoefer. SeBS: A serverless benchmark suite for function-as-a-service computing. In *Proceedings of the 22nd International Middleware Conference (Middleware '21)*, Québec city, Canada, December 2021.
- [22] Marcin Copik, Konstantin Taranov, Alexandru Calotoiu, and Torsten Hoefer. rFaaS: RDMA-enabled FaaS platform for serverless high-performance computing. *arXiv preprint arXiv:2106.13859*, 2021.
- [23] Datadog. The state of serverless, May 2021. <https://www.datadoghq.com/state-of-serverless/>.
- [24] Vojislav Dukic, Rodrigo Bruno, Ankit Singla, and Gustavo Alonso. Photons: Lambdas on a diet. In *Proceedings of the 11th ACM Symposium on Cloud Computing (SoCC '20)*, Virtual, October 2020.
- [25] Simon Eismann, Long Bui, Johannes Grohmann, Cristina Abad, Nikolas Herbst, and Samuel Kounev. Sizeless: Predicting the optimal size of serverless functions. In *Proceedings of the 22nd International Middleware Conference (Middleware '21)*, New York, NY, May 2021. ACM.
- [26] Simon Eismann, Long Bui, Johannes Grohmann, Cristina Abad, Nikolas Herbst, and Samuel Kounev. Sizeless: Predicting the Optimal Size of Serverless Functions (Middleware '21). In *Proceedings of the 22nd International Middleware Conference*, Québec city, Canada, 2021.
- [27] Peter X. Gao, Akshay Narayan, Sagar Karandikar, Joao Carreira, Sangjin Han, Rachit Agarwal, Sylvia Ratnasamy, and Scott Shenker. Network Requirements for Resource Disaggregation. In *12th USENIX Symposium on Operating Systems Design and Implementation (OSDI '16)*, Savannah, GA, October 2016.
- [28] Robert Grandl, Ganesh Ananthanarayanan, Srikanth Kandula, Sriram Rao, and Aditya Akella. Multi-Resource Packing for Cluster Schedulers. *SIGCOMM Comput. Commun. Rev.*, 44(4):455–466, aug 2014.
- [29] Juncheng Gu, Youngmoon Lee, Yiwen Zhang, Mosharaf Chowdhury, and Kang Shin. Efficient Memory Disaggregation with Infiniswap. In *Proceedings of the 14th USENIX Symposium on Networked Systems Design and Implementation (NSDI '17)*, Boston, MA, April 2017.
- [30] Hewlett Packard. The Machine: A New Kind of Computer. <http://www.hpl.hp.com/research/systems-research/themachine/>, 2005.
- [31] Jun Rao Jay Kreps, Neha Narkhede. Kafka: A distributed messaging system for log processing. In *Proceedings of the 6th International Workshop on Networking Meets Databases (NetDB '11)*, Athens, Greece, June 2011.
- [32] Eric Jonas, Qifan Pu, Shivaram Venkataraman, Ion Stoica, and Benjamin Recht. Occupy the cloud: Distributed computing for the 99%. In *Proceedings of the 2017 Symposium on Cloud Computing (SoCC '17)*, Santa Clara, CA, September 2017.
- [33] Ana Klimovic, Yawen Wang, Patrick Stuedi, Animesh Trivedi, Jonas Pfefferle, and Christos Kozyrakis. Pocket: Elastic ephemeral storage for serverless analytics. In *13th USENIX Symposium on Operating Systems Design and Implementation (OSDI '18)*, Carlsbad, CA, October 2018.
- [34] AWS Lambda. Configuring Lambda function memory, Accessed 2021-12-13. <https://docs.aws.amazon.com/lambda/latest/dg/configuration-memory.html>.
- [35] Huaicheng Li, Daniel S. Berger, Stanko Novakovic, Lisa Hsu, Dan Ernst, Pantea Zardoshti, Monish Shah, Samir Rajadnya, Scott Lee, Ishwar Agarwal, Mark D. Hill, Marcus Fontoura, and Ricardo Bianchini. Pond: CXL-Based Memory Pooling Systems for Cloud Platforms, 2022.
- [36] Ashraf Mahgoub, Edgardo Barsallo Yi, Karthick Shankar, Sameh Elnikety, Somali Chaterji, and Saurabh Bagchi. ORION and the Three Rights: Sizing, Bundling, and Prewarming for Serverless DAGs. In *16th USENIX Symposium on Operating Systems Design and Implementation (OSDI' 22)*, Carlsbad, CA, July 2022.
- [37] Anup Mohan, Harshad Sane, Kshitij Doshi, Saikrishna Edupuganti, Naren Nayak, and Vadim Sukhomlinov. Agile cold starts for scalable serverless. In *11th USENIX Workshop on Hot Topics in Cloud Computing (HotCloud '19)*, Renton, WA, July 2019.
- [38] Djob Mvondo, Mathieu Bacou, Kevin Nguetchouang, Lucien Ngale, Stéphane Pouget, Josiane Kouam, Renaud Lachaize, Jinho Hwang, Tim Wood, Daniel Hagimont, et al. OFC: an opportunistic caching system for FaaS platforms. In *Proceedings of the Sixteenth European Conference on Computer Systems (EuroSys '21)*, Virtual, April 2021.
- [39] Joe H. Novak, Sneha Kumar Kasera, and Ryan Stutsman. Cloud functions for fast and robust resource auto-scaling. In *2019 11th International Conference on Communication Systems and Networks (COMSNETS)*, pages 133–140, 2019.

- [40] John Ousterhout, Arjun Gopalan, Ashish Gupta, Ankita Kejriwal, Collin Lee, Behnam Montazeri, Diego Ongaro, Seo Jin Park, Henry Qin, Mendel Rosenblum, Stephen Rumble, Ryan Stutsman, and Stephen Yang. The ramcloud storage system. *ACM Transactions Computer System*, 33(3):7:1–7:55, August 2015.
- [41] Meikel Poess, Bryan Smith, Lubor Kollar, and Paul Larson. Tpc-ds, taking decision support benchmarking to the next level. In *Proceedings of the 2002 ACM SIGMOD international conference on Management of data (SIGMOD '02)*, Madison, Wisconsin, June 2002.
- [42] Qifan Pu, Shivaram Venkataraman, and Ion Stoica. Shuffling, fast and slow: Scalable analytics on serverless infrastructure. In *16th USENIX Symposium on Networked Systems Design and Implementation (NSDI '19)*, Boston, MA, February 2019.
- [43] redislabs. Redis. <https://redis.io/>, 2009.
- [44] Francisco Romero, Gohar Irfan Chaudhry, Íñigo Goiri, Pragna Gopa, Paul Batum, Neeraja J. Yadwadkar, Rodrigo Fonseca, Christos Kozyrakis, and Ricardo Bianchini. FaaS\$T\$: A transparent auto-scaling cache for serverless applications. In *Proceedings of the ACM Symposium on Cloud Computing (SoCC '21)*, New York, NY, November 2021.
- [45] Rohan Basu Roy, Tirthak Patel, and Devesh Tiwari. IceBreaker: Warming serverless functions better with heterogeneity. In *Proceedings of the 27th ACM International Conference on Architectural Support for Programming Languages and Operating Systems (ASPLOS '22)*, Lausanne, Switzerland, April 2022.
- [46] Zhenyuan Ruan, Malte Schwarzkopf, Marcos K. Aguilera, and Adam Belay. AIFM: High-Performance, Application-Integrated Far Memory. In *14th USENIX Symposium on Operating Systems Design and Implementation (OSDI '20)*, Banff, Canada, November 2020.
- [47] Mohammad Shahradd, Rodrigo Fonseca, Íñigo Goiri, Gohar Chaudhry, Paul Batum, Jason Cooke, Eduardo Laureano, Colby Tresness, Mark Russinovich, and Ricardo Bianchini. Serverless in the wild: Characterizing and optimizing the serverless workload at a large cloud provider. In *2020 USENIX Annual Technical Conference (ATC '20)*, Virtual, July 2020.
- [48] Yizhou Shan, Yutong Huang, Yilun Chen, and Yiyang Zhang. LegoOS: A Disseminated, Distributed OS for Hardware Resource Disaggregation. In *Proceedings of the 13th USENIX Symposium on Operating Systems Design and Implementation (OSDI '18)*, Carlsbad, CA, October 2018.
- [49] Craig Shoemaker, Jeff Hollan, David Coulter, Daniel Cazzulino, Alex Mang, Andy J, and Glenn Gaiety. Azure Functions reliable event processing, May 2020. <https://docs.microsoft.com/en-us/azure/azure-functions/functions-reliable-event-processing>.
- [50] Arjun Singhvi, Arjun Balasubramanian, Kevin Houck, Mohammed Danish Shaikh, Shivaram Venkataraman, and Aditya Akella. Atoll: A scalable low-latency serverless platform. In *Proceedings of the ACM Symposium on Cloud Computing (SoCC '21)*, Seattle, WA, November 2021.
- [51] Vikram Sreekanti, Chenggang Wu, Xiayue Charles Lin, Johann Schleier-Smith, Joseph E Gonzalez, Joseph M Hellerstein, and Alexey Tumanov. Cloudburst: Stateful functions-as-a-service. In *Proceedings of the VLDB Endowment (VLDB '20)*, Tokyo, Japan, August 2020.
- [52] Shelby Thomas, Lixiang Ao, Geoffrey M. Voelker, and George Porter. Particle: Ephemeral endpoints for serverless networking. In *Proceedings of the 11th ACM Symposium on Cloud Computing (SoCC '20)*, New York, NY, October 2020.
- [53] Shin-Yeh Tsai, Yizhou Shan, , and Yiyang Zhang. Disaggregating Persistent Memory and Controlling Them from Remote: An Exploration of Passive Disaggregated Key-Value Stores. In *Proceedings of the 2020 USENIX Annual Technical Conference (ATC '20)*, Boston, MA, USA, July 2020.
- [54] Ao Wang, Jingyuan Zhang, Xiaolong Ma, Ali Anwar, Lukas Rupperecht, Dimitrios Skourtis, Vasily Tarasov, Feng Yan, and Yue Cheng. InfiniCache: Exploiting ephemeral serverless functions to build a cost-effective memory cache. In *18th USENIX Conference on File and Storage Technologies (FAST '20)*, Santa Clara, CA, February 2020.
- [55] Xingda Wei, Fangming Lu, Rong Chen, and Haibo Chen. KRCORE: A microsecond-scale RDMA control plane for elastic computing. In *2022 USENIX Annual Technical Conference (USENIX ATC 22)*, pages 121–136, Carlsbad, CA, July 2022. USENIX Association.
- [56] Xingda Wei, Tianxia Wang, Jinyu Gu, Yuhang Yang, Fangming Lu, Rong Chen, and Haibo Chen. Booting 10k serverless functions within one second via RDMA-based remote fork. *arXiv preprint arXiv:2203.10225*, 2022.
- [57] Wes McKinney. Data Structures for Statistical Computing in Python. In *Proceedings of the 9th Python in Science Conference (SciPy '10)*, Austin, Texas, June 2010.

- [58] Chenggang Wu, Vikram Sreekanti, and Joseph M. Hellerstein. Transactional Causal Consistency for Serverless Computing. In *Proceedings of the 2020 ACM SIGMOD International Conference on Management of Data (SIGMOD '20)*, Portland, OR, USA, 2020.
- [59] Fei Xu, Yiling Qin, Li Chen, Zhi Zhou, and Fangming Liu. λ dnn: Achieving predictable distributed dnn training with serverless architectures. *IEEE Transactions on Computers*, 71(2):450–463, 2021.
- [60] Tian Zhang, Dong Xie, Feifei Li, and Ryan Stutsman. Narrowing the Gap Between Serverless and its State with Storage Functions. In *Proceedings of the ACM Symposium on Cloud Computing (SoCC'19)*, SoCC'19. ACM, 2019.
- [61] Wen Zhang, Vivian Fang, Aurojit Panda, and Scott Shenker. Kappa: a programming framework for serverless computing. In *Proceedings of the 11th ACM Symposium on Cloud Computing (SoCC '20)*, Virtual, October 2020.